Research in Astronomy and Astrophysics, 25:025003 (7pp), 2025 February

https://doi.org/10.1088/1674-4527/ad7365
CSTR: 32081.14.RAA.ad7365

The Stellar Abundances and Galactic Evolution Survey (SAGES) III

Chun Li[1], Zhou Fan[1,2], Gang Zhao[1,2], Wei Wang[1], Jie Zheng[1], Kefeng Tan[1], Jingkun Zhao[1], Yang Huang[1], Haibo Yuan[2], Kai Xiao[1,2], Yuqin Chen[1], Haining Li[1], Yujuan Liu[1], Nan Song[1,3], Ali Esamdin[4], Hu-Biao Niu[4], Jin-Zhong Liu[4], and Guo-Jie Feng[4]
[1] CAS Key Laboratory of Optical Astronomy, National Astronomical Observatories, Chinese Academy of Sciences, Beijing 100101, China; lichun@nao.cas.cn, zfan@nao.cas.cn, gzhao@nao.cas.cn
[2] School of Astronomy and Space Science, University of Chinese Academy of Sciences, Beijing 100049, China
[3] China Science and Technology Museum, Beijing 100101, China
[4] Xinjiang Astronomical Observatory, Urumqi 830011, China
Received 2023 December 29; revised 2024 July 24; accepted 2024 August 17; published 2025 January 22

Abstract

The Stellar Abundances and Galactic Evolution Survey (SAGES) is a multi-band survey that covers the northern sky area of ∼12,000 deg2. The Nanshan One-meter Wide-field Telescope (NOWT) of the Xinjiang Astronomical Observatory carried out observations on $g/r/i$ bands. Here, we present the survey strategy, data processing, catalog construction, and database schema. The observations of NOWT started in 2016 August and were completed in 2018 January, a total of 17,827 frames were obtained and ∼4600 deg2 sky areas were covered. In this paper, we release the catalog of the data in the $g/r/i$ bands observed by NOWT. In total, there are 109,197,578 items of source records. The catalog is the supplement for the SDSS for the bright end, and the combination of our catalog and these catalogs could be helpful for source selections for other surveys and Milky Way sciences, e.g., white dwarf candidates and stellar flares.

Key words: surveys – catalogs – techniques: photometric

1. Introduction

Astronomy is a science based on observation. Large field sky surveys are of great significance to the study of the structure and evolution of the galaxy. In recent decades, massive discoveries have been made based on a lot of sky survey projects such as Gaia, LAMOST, GSC, 2MASS, etc. SkyMapper is a southern sky survey that is efficient at identifying metal-poor stars. Hence we have launched a similar project, Stellar Abundances and Galactic Evolution Survey (SAGES) for the northern sky area.

The SAGES is a multi-band survey that covers the northern sky. The Nanshan One-meter Wide-field Telescope (NOWT) of the Xinjiang Astronomical Observatory (XAO), Chinese Academy of Sciences (CAS) carried out observations on $g/r/i$ passbands. Here, we present the survey strategy, data processing, catalog construction, and database schema. The observation of NOWT started in 2016 August and was completed in 2018 January, a total of 17,827 frames were obtained and ∼4600 deg2 sky areas were covered.

SAGES is a northern sky photometry survey with eight passbands, that intends mainly to search for metal-poor stars in the Galaxy (Fan et al. 2023). The survey aims to derive stellar atmospheric parameters for a few hundred million stars. The SAGES photometric system is unique and defined by the SAGES team, which is composed of eight bands (the $u_s/v_s/g/r/i/\alpha_n/\alpha_w$/DDO51), including narrow-band, intermediate bands, and broad bands as well. The sky coverage of the project covers the northern sky region of decl. $\delta > -5°$ and avoids the Galactic disk region of $-10° < b < +10°$ while avoiding saturation and image contamination that may result from excessive bright stars. The designed survey area was larger than 12,000 deg2 (∼60% of the northern sky). Since the beginning of operation in 2016, data has been obtained for five bands. Among them, the u_s and v_s bands catalog has been released by Fan et al. (2023). The $g/r/i$ bands were observed by NOWT, data of 4254 sky areas was covered, and 17,827 frames were obtained. After data reduction, photometry, calibration, and data combination, 51,149,452 sources were detected. The complete magnitudes for $g/r/i$ passbands are 19.2 mag, 19.1 mag, and 18.2 mag, respectively. This part of the data has been released and is available on the China-VO platform.

This paper briefly introduces the observation data of Nanshan $g/r/i$ bands in SAGES. The second section will introduce the basic situation of the project. The observation detail will be shown in Section 3. The data reduction processing will be described in Section 4. In Section 5 we show the data quality, and the summary and future plans are in Section 6.

2. Nanshan DATA of SAGES Photometric System

2.1. The Photometric System of SAGES

Figure 1 and Table 1 present the details of the eight passbands of SAGES. The u_s is similar to the one in the

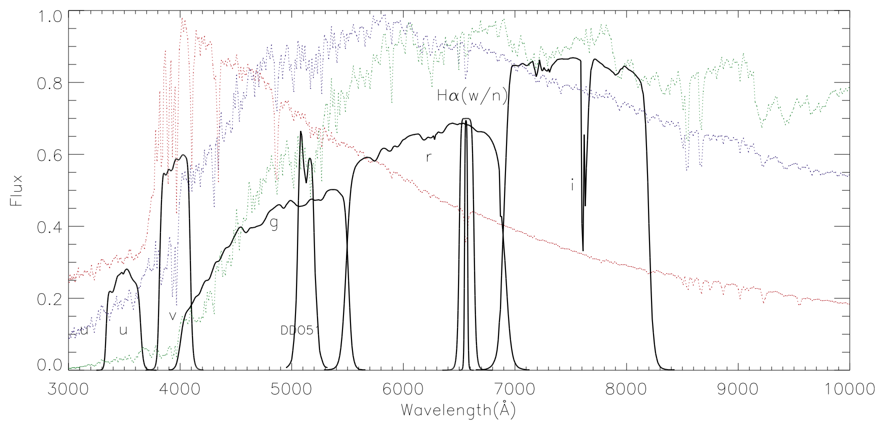

Figure 1. The filter response functions of SAGES photometric system, overplotted with the spectra of typical F-stars (red) G-stars (blue) K-stars (green).

Table 1
SAGES Photometry System

Band	u_s	v_s	g	r	i	DDO51	α_w	α_n
wavelength (Å)	3520	3950	4639	6122	7439	5132	6563	6563
width (Å)	314	290	1280	1150	1230	162	29	136

Strömgren–Crawford (SC) system which covers the Balmer jump, and v_s is a self-developed filter that covers the Ca II H&K absorption lines, which are very sensitive to the metallicity of stars. Therefore, the two passbands have a good identification function for metal-poor stars. The other three bands, $g/r/i$ are the same as SDSS passbands, which are useful in estimating the effective temperature $T_{\rm eff}$ of stars. The observation plan made for $g/r/i$ in SAGES mainly intends to complete the coverage of the whole north sky with the combination of the SDSS catalog. The DDO51 band is sensitive to the gravity of late-type stars. Another two bands, α_n and α_w, are used to estimate the interstellar extinctions, as the value of $\alpha_w - \alpha_n$ is only sensitive to the effective temperature $T_{\rm eff}$, and is independent of interstellar extinction. Thus the effective temperature $T_{\rm eff}$ is easy to constrain more accurately. Then the difference between them and $T_{\rm eff}$ from other colors carried constrains for extinction. DDO51 measures the MgH feature in KM dwarfs (Bessell 2005). For further information about SAGES please refer to Fan et al. (2023).

2.2. The Overall Observation Progress of the SAGES Project

The observation of eight bands of SAGES is processed in different telescopes and sites.

The u_s and v_s bands are observed at the Kitt Peak National Observatory (KPNO) in Arizona, USA, with a 90-inch Bok telescope.

Because of the lack of observation time from February to August and weather conditions, the sky area of $12 < \alpha < 18$ hr of R.A is not included in the survey. The u/v passband data has been released by Fan et al. 2023.

Observations of $g/r/i$ passbands have already been carried out by NOWT since 2016 August and ended in 2018 January, with part of the data introduced in this paper.

From the plan of DDO51, α_w and α_n passbands, multiple telescopes were intended for use, including a 1 m Zeiss telescope of Maidanak astronomical observatory (MAO, 66° 53′47″E, 38°40′22″N), which belongs to Ulugh Beg Astronomical Institute (UBAI), Uzbekistan (Kardopolov & Filip'ev 1979), and Xuyi 1 m Schmidt telescope of the Purple Mountain Observatory (PMO) of CAS.

Observation of the DDO51 passband with the telescope of NOWT is still ongoing. The observations of the whole sky coverage of SAGES will be completed in 3 yr (2023–2026).

2.3. Observatory and Telescope

The NOWT belongs to XAO, CAS, which is located in the Nanshan Observatory (87°10′30″E, 43°28′25″N), which is ~75 km away from Urumqi city, with an altitude of 2088 meters (Bai et al. 2000). The observable night of Nanshan Station is more than 300 days per year, and the clear night is greater than 210 days. The distribution peak of seeing values around 1.″67, and 80% of the values obtained at night are below 2.2. At the zenith, the sky brightness is around 21.7 mag arcsec^{-2} in the V-band (Bai et al. 2000).

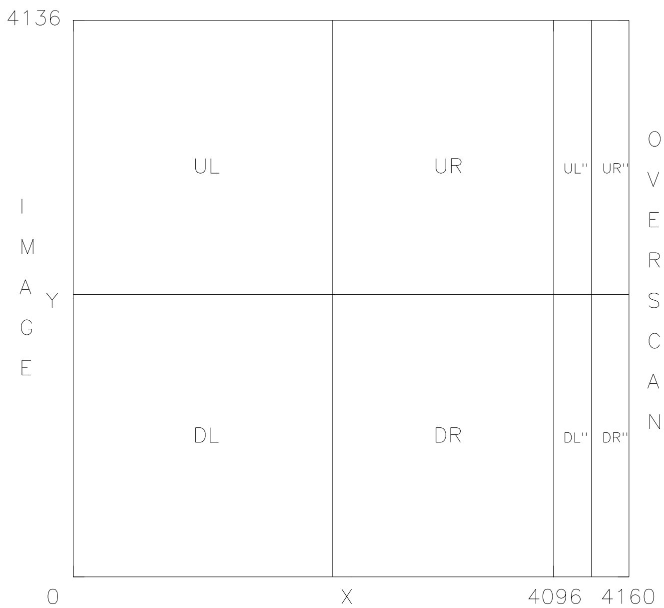

Figure 2. The Andor 4 k × 4 k NOWT CCD array, shows four amplifiers. The right side shows an overscan area.

NOWT is a one-meter telescope with an Alt-Az mount, operating at prime focus with a field corrector. The parabolic primary mirror's effective diameter is 1 m and the focal length is 2159 ± 20 mm (Bai et al. 2000). Pointing accuracy is better than $3''$ (rms-error), tracking accuracy is $1\farcs8$ rms in 60 minutes (Bai et al. 2000).

Totally, 80% of the collected energy is concentrated into a circle with a diameter of less than $1\farcs15$ on a field diameter of $2\fdg4$. The pointing accuracy for this telescope is better than $5''$ rms for each axis after pointing model correction (Liu et al. 2013; Bai et al. 2000).

The NOWT provides excellent optical quality in photometry which is a great benefit for SAGES.

2.4. Detectors of Nanshan g/r/i Observation

The filters for the $g/r/i$ passbands used in NOWT for SAGES were made by Custom Scientific, Inc., USA, which is the standard SDSS system.

The CCD camera installed on NOWT was 4096×4136 pixels, designed and integrated by the CCD laboratory of NAOC (Bai et al. 2000). The camera was placed at the prime focus of the telescope and cooled by liquid nitrogen. The camera has four amplifiers for fast readout, which is shown in Figure 2. The physical size of the pixel was 12×12 μm, with the given field of view $1.3° \times 1.3°$, and a pixel scale of $1\farcs124$ (Bai et al. 2000).

For the overscan, as we can see in Figure 2, 32-pixel columns in total are set under scan pixels for each amplifier, which is used to correct image data for bias.

2.5. Observations

The planned survey area was given in Section 1. The $g/r/i$ bands of the mission are mainly to complete the sky area of the SDSS survey and SAGES. Because of the latitude of NOWT and telescope location, the sky areas only for decl. $> 5°$ were observed.

2.6. Observing Strategy and Coverage

The field of view of NOWT is $\sim 1\fdg3 \times 1\fdg3$, so we have designed each survey field as $1\fdg04 \times 1\fdg04$. Thus, the designed $\sim$4600 deg2 sky area was divided into 4254 blocks for observation. The fields on the same decl. are called a stripe, and the adjacent five fields are combined as a survey block, so we will reduce the long moving between blocks. The overlap area between neighbor fields will help in the flux calibration and ensure the coverage of the whole sky. We named each field with an integer sequence. Since SDSS had covered a large area of the southern sky, we need only to finish the rest. The blocks of NOWT are displayed in Figure 3.

We have developed a strategy pipeline that helps to generate observation scripts for each night. The pipeline works in these ways: ensuring no duplicated observation of each field, choosing proper blocks according to the observation date, excluding the fields near the moon, and sorting the blocks to make sure airmass will be minimum. The pipeline will also provide the animated progress of observations so we can check our observation progress. If the observation was interrupted by bad weather or other opportunity targets, the report of the pipeline will help the operators resume from a proper position.

3. Data Reduction

3.1. Image Correction

One pipeline was built for the photometry and astrometry steps by our team. The data correction procedure includes overscan correction, biases combination, flats combination, and survey image correction. Twilight flats are used for correction in NOWT runs.

For overscans, the median value of each row was subtracted. For bias, we took a set of 10 bias images before and after observation, and used the median of the bias for correction. Then all survey images and flat-field images process bias removal.

For flats, a set of 10 skylight flat frames for each band was taken before and after observation, if weather allowed. After removing of bias, the flat images were normalized and combined with median values.

The survey images are executed through overscan correction, bias removal, and flat correction procedures.

The numbers of images after correction are 5283 frames in the g band, 4849 frames in the r band, and 5314 frames in the i band.

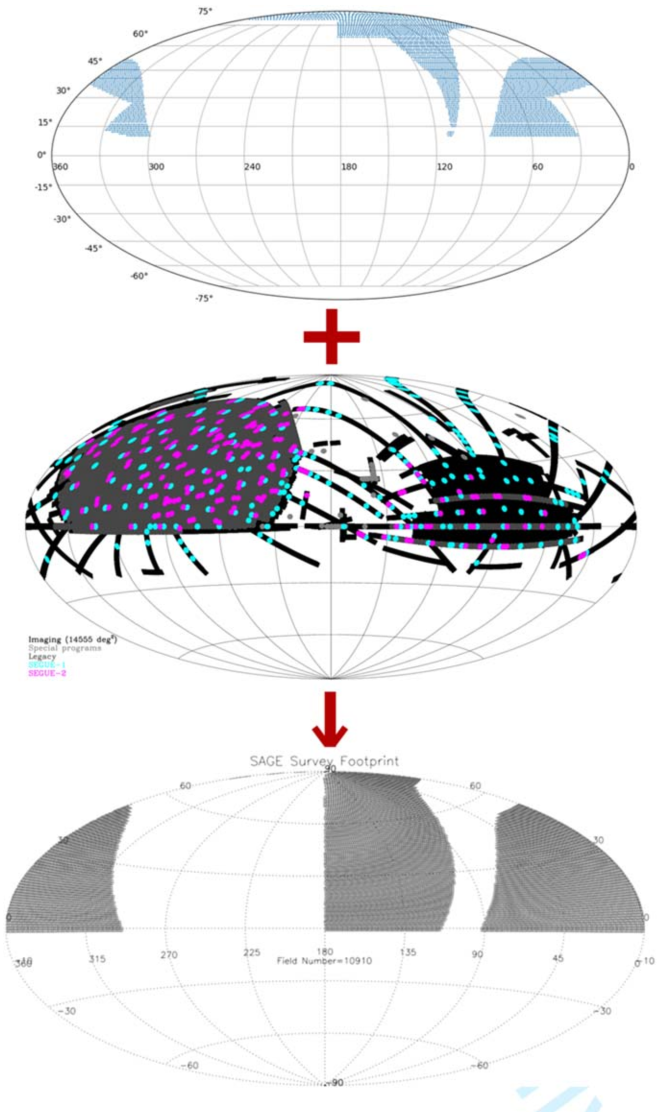

Figure 3. The sky coverage for SAGES in $g/r/i$ passbands. The designed area can be combined with the SDSS data for the completeness of the catalog, including 4254 blocks. The upper panel presents the designed area of $g/r/i$ passbands, the middle panel shows the SDSS Legacy Sky Coverage (https://www.sdss4.org/dr17/), and the bottom panel is the sky coverage of the whole SAGES project.

Table 2
Parameters of Output Catalog

SAGE_ID	ID for SAGES
RA	Right ascension of object (J2000)
DED	Declination of the object (J2000)
MAG_G/R/I	Magnitude in the $g/r/i$ passband
ERR_G/R/I	Error of magnitude in $g/r/i$ passband
OBS_TIME_G/R/I	Time of observation of certain frame
FLAG_G/R/I	Flag from Source Extractor of certain frame

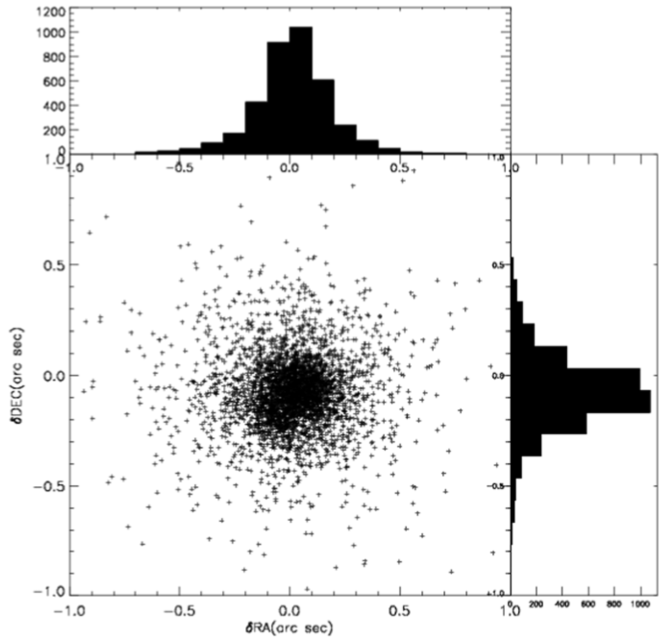

Figure 4. The precision of astrometry for the Nanshan run. The external astrometric errors are estimated by comparing the difference between the coordinates of one typical image (named n8037.0172 of the g band) and those from reference catalog PS1.

The tool Source Extractor (SE) (Bertin & Armouts 1996) was used to detect the sources and perform photometry. Astrometry tool Scamp (Software for Calibrating AstroMetry and Photometry) (Bertin 2006) was used for the astrometric procedure. Both SE and SCAMP are well-developed and widely used in data reduction of photometry surveys. The Position and Proper Motion Extended (PPMX) (Roser et al. 2008) catalog is adopted as the astrometric reference for its relatively good accuracy (Zheng et al. 2018, 2019).

We run SE for the corrected images using the position information in the fits head to produce a preliminary source catalog Then we run SCAMP twice with different parameters to get more precise astrometry results. With the WCS information, we run SE again to obtain a catalog of instrumental magnitude. The output parameter Mag_Auto of SE was used as the primary instrumental magnitude.

The data fields of the final local catalog of each image are listed in Table 2. The FLAG_G/R/I are the standard SE flags. For details of flags please refer to Fan et al. (2023) and Bertin & Armouts (1996).

3.2. Flux Calibration

Xiao et al. (2023a) utilized both the spectroscopy-based Stellar Color Regression method (SCR method; Yuan et al. 2015) and the photometric-based SCR method (SCR′ method)

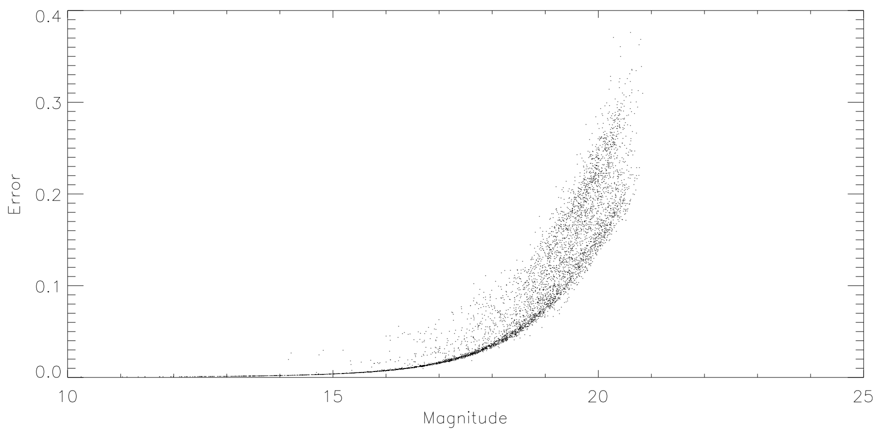

Figure 5. The photometric uncertainties (from Poisson statistics) vs. magnitude in the Nanshan run for one typical image named n7634.0303. The limiting magnitude is ∼16.5 mag, with uncertainties of 0.01 mag, which corresponds to S/N ∼ 100.

to construct a total of approximately 2.6 million dwarfs as standard stars, achieving an accuracy of about 0.01–0.02 mag per band. They then performed relative photometric calibration of the NOWT's $g/r/i$ bands imaging data. Absolute calibration was conducted using the corrected Pan-STARRS DR1 (PS1) photometry by Xiao & Yuan (2022) and Xiao et al. (2023b), establishing the transformation relationship between the calibrated magnitudes from the NOWT and the corrected PS1 magnitudes. A comprehensive analysis of repeated sources in adjacent images revealed a remarkable internal consistency of approximately 1–2 mmag across all filters. By employing the synthetic photometry method with Gaia DR3 BP/RP spectra, the PS1 magnitudes were synthesized, resulting in a photometric calibration uniformity of approximately 2.4 mmag, 2.3 mmag, and 0.9 mmag photometric calibration uniformity for the $g/r/i$ bands, respectively, within each field with a diameter of 1°.3. During the photometric calibration process, the dependence of the CCD gain and stellar flat on the observation time is discussed, as well as the CCD position-dependent residual of stellar flat correction. More details can be found in Xiao et al. (2023a) and Fan et al. (2023).

4. Data Quality

In the Nanshan part of the data, the count of g passband images involved in calibration was 5096, 4551 fro the r passband, and 5153 for the i passband. The total count of survey images is 14,800.

The total sources detected are 31,894,325 in the g band, 38,711,424 in the r band, and 38,531,820 in the i band. After a combination of all sources, we have 51,149,452 sources in total. Among them, 21,819,140 were detected in all $g/r/i$ passbands.

4.1. Astrometry Precision

Figure 4 presents the typical astrometric error. The data is from one frame named n8037.0172 in the g band. The external astrometric errors are estimated by comparing the difference between the coordinates of one typical image and those from reference catalog PS1. The rms of the difference between the coordinates (calculated from all detected sources) is 0.″28 for the g band, 0.″29 for the r band, and 0.″30 for the i band, which are good enough for the WCS and astrometry.

4.2. The Limiting Magnitudes

Figure 5 shows a typical magnitude versus photometric error diagram in the r band. The photometric error is from Poisson statistics, not including the calibration errors. We can see that the limiting magnitude of S/N ∼ 10(uncertainty of 0.1) is ∼19.0. The scatter is due to the local background fluctuation which may be caused by contamination of nearby sources and nonuniformity of skylight background.

The limiting magnitudes reach 16.57, 16.46, and 15.49 mag in the $g/r/i$ bands, respectively, with an uncertainty of 0.01 mag, which is the Poisson error, not including the flux calibration errors (internal calibration and zero-point). We use all the frames to calculate the limit mag then use the median value for each band. The limiting magnitudes for the uncertainty of 0.2 mag (corresponding to S/N = 5) are 20.19, 20.03, and 19.18, respectively. Figure 6 shows the limit magnitude distribution for all fields of the g band for S/N = 100, corresponding to the photometry error of 0.01 mag.

Figure 7 is the magnitude distribution for $g/r/i$ passbands. From the turning point of the diagrams, the complete magnitudes for $g/r/i$ passbands are 19.2, 19.1, and 18.2 mag, respectively, which show the depth of observation.

Figure 8 shows the magnitude distribution for all the sources of the Nanshan run of SAGES in all observed fields of $g/r/i$ passbands, respectively. The x-axis is the magnitude range and the y-axis represents the counts for the photometry magnitude number. It can be seen that the peaks are $g \sim 19.2$ mag and

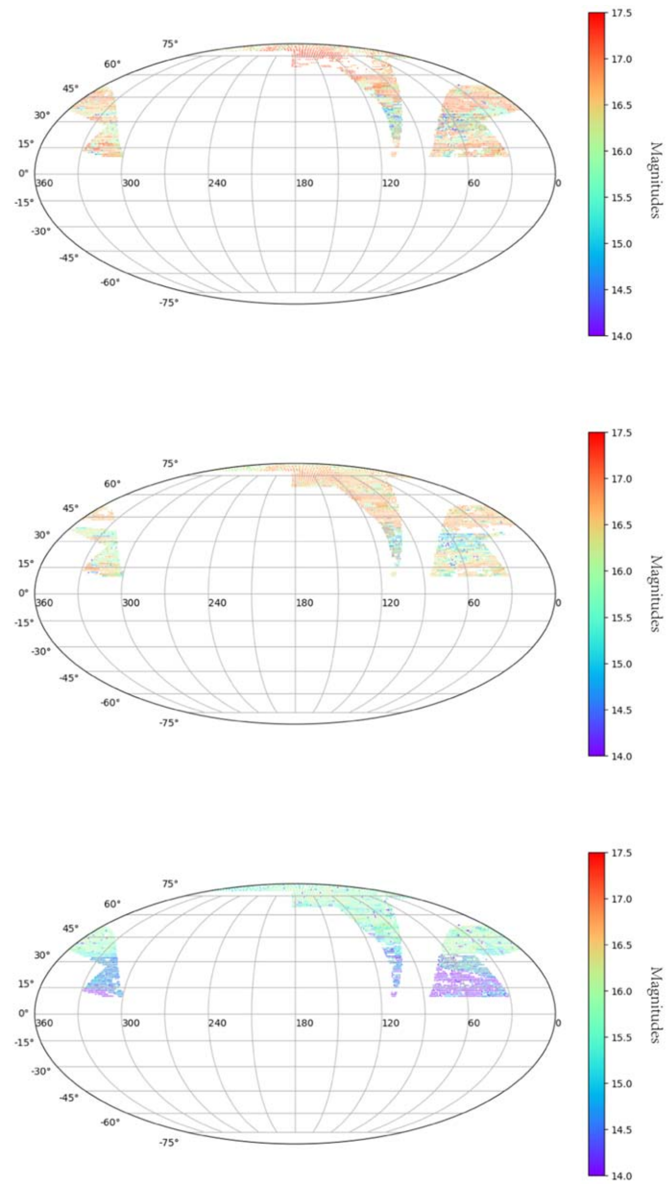

Figure 6. Magnitude distribution for all fields of g (upper panel), r (second panel), and r (bottom panel) passbands for S/N = 100, corresponding to the photometry error of 0.01 mag. The median magnitude is 16.57, 16.46, and 15.49 mag, respectively.

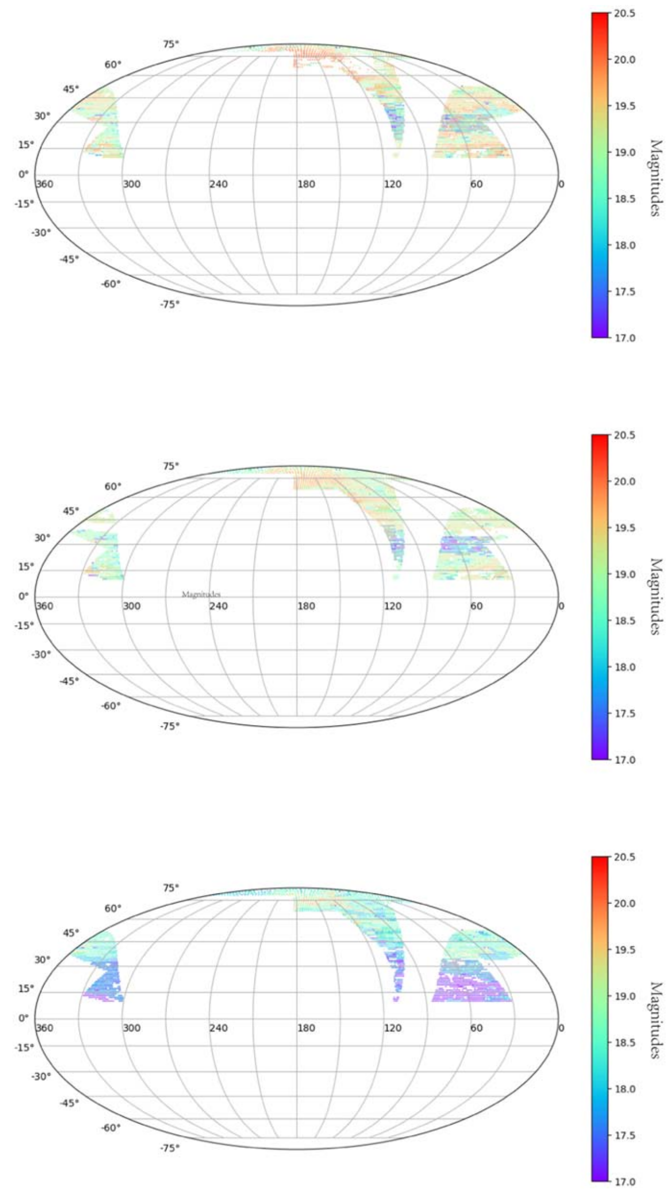

Figure 7. Magnitude distribution of g (upper panel), r (second panel), and r (bottom panel) passbands but for complete magnitudes. The median complete magnitude is 19.2 mag, 19.1 mag, and 18.2 mag, respectively.

$r \sim 19.1$ mag and $i \sim 18.2$ mag for the Nanshan observing run of SAGES, which correspond to the complete magnitude.

5. Data Access

SAGES $g/r/i$ data has been released and is available on the China-VO platform and the National Astronomical Data Center (NADC) https://nadc.china-vo.org.

6. Summary and Future Plans

This paper presents part of the whole SAGES, the observing strategy, observation, data reduction, and catalog production of SAGES $g/r/i$ passband which is processed with NOWT.

Some of the data reduction and calibration process steps will be upgraded. For instance, the removal of the fringe of i band images. We hope this will help to improve the photometry and calibration, and provide us with a deeper detection and more precise data.

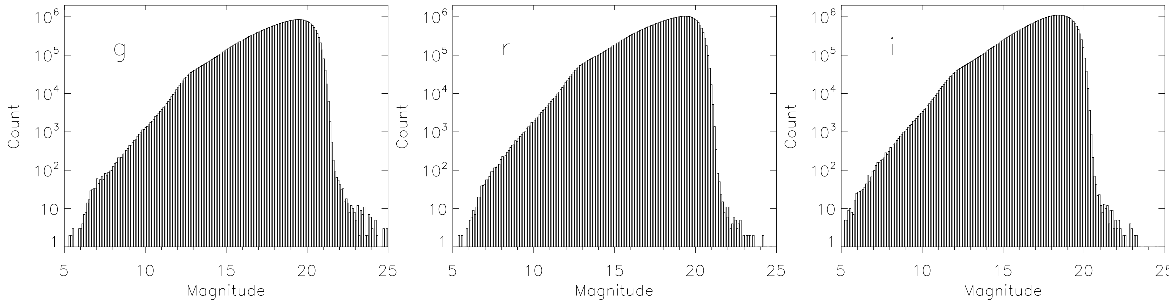

Figure 8. The magnitude distribution for all the sources of the Nanshan run of SAGES in all observed fields of $g/r/i$ passbands, respectively. The x-axis is the magnitude range and the y-axis represents the counts for the photometry magnitude number. The peaks are $g\sim 19.2$ mag, $r\sim 19.1$ mag, and $i\sim 18.2$ mag.

The observation of other passbands of SAGES (DDO51 and α_w) will be completed in the next few years. Further works of SAGES will contain more passbands, more images, and better sky coverage.

Acknowledgments

This study is supported by the National Natural Science Foundation of China (NSFC) under grant Nos. 12261141689, 12090044, and 12090040. This study is also sponsored by the Xinjiang Uygur Autonomous Region "Tianchi Talent" Introduction Plan.

The Stellar Abundance and Galactic Evolution Survey (SAGES) is a multi-band photometric project built and managed by the Research Group of the Stellar Abundance and Galactic Evolution of the National Astronomical Observatories, Chinese Academy of Sciences (NAOC).

ORCID iDs

Chun Li https://orcid.org/0009-0000-4835-7525
Zhou Fan https://orcid.org/0000-0002-6790-2397
Wei Wang https://orcid.org/0000-0002-9702-4441
Jie Zheng https://orcid.org/0000-0001-6637-6973
Kefeng Tan https://orcid.org/0000-0003-0173-6397

References

Bai, C., Feng, G., Zhang, X., et al. 2000, RAA, 20, 211
Bessell, M. S. 2005, ARA&A, 43, 293
Bertin, E., & Armouts, S. 1996, A&AS, 117, 393
Bertin, E. 2006, in ASP Conf. Ser. 351, Astronomical Data Analysis Software and Systems XV, ed. C. Gabriel et al. (San Francisco, CA: ASP), 112
Fan, Z., Zhao, G., Wang, W., et al. 2023, ApJS, 268, 9
Kardopolov, V. I., & Filip'ev, G. K. 1979, SvAL, 5, 58
Liu, J.-Z., Zhang, Y., Feng, G.-J., & Bai, C.-H. 2013, in IAU Symp. 298, Setting the Scene for Gaia and LAMOST, ed. S. Feltzing (Cambridge: Cambridge Univ. Press), 427
Roser, S., Schilbach, E., Schwan, H., et al. 2008, A&A, 488, 401
Xiao, K., & Yuan, H. 2022, AJ, 163, 185
Xiao, K., Yuan, H., Huang, B., et al. 2023a, ChSBu, 68, 2790
Xiao, K., Yuan, H., Huang, B., et al. 2023b, ApJS, 268, 53
Yuan, H.-B., Liu, X.-W., Xiang, M.-S., et al. 2015, ApJ, 799, 133
Zheng, J., Zhao, G., Wang, W., et al. 2018, RAA, 18, 147
Zheng, J., Zhao, G., Wang, W., et al. 2019, RAA, 19, 3